

Quasi-isothermal superfluid-film flow: Oscillations between two reservoirs*

Robert B. Hallock† and Ephraim B. Flint

Department of Physics and Astronomy, University of Massachusetts, Amherst, Massachusetts 01002

(Received 16 April 1974)

We have carried out a detailed study of the frequency and damping of the oscillations in levels of two reservoirs of HeII which are coupled only via the mobile superfluid film. Our experiments cover the temperature range $1.2 < T < 2.13$ K and utilize several geometries under quasi-isothermal conditions. Below 2 K our results for the damping are in quantitative agreement with predictions based on a theory first proposed by Robinson. This indicates that the damping mechanisms proposed by Allen and by Calvani, Greulich, and Maraviglia are of minor importance under our experimental conditions. It is argued that the Robinson theory can explain the previous general agreement with the Allen theory.

I. INTRODUCTION

Consider a reservoir containing He II which is coupled only by the superfluid film to a second reservoir also containing He II. As is well known, the application of a chemical-potential difference between the two reservoirs will result in mass transport via the film which will serve to reduce the applied chemical-potential difference. Various methods, for example, the imposition of a temperature difference or a level difference may be used to create a difference in chemical potential. At the end of the flow which acts to remove the relative potential difference, the level in each reservoir will oscillate about its new equilibrium value. The damping constant and frequency of these oscillations form the subject of the present study.

These oscillations were first studied in detail by Atkins.¹ He derived an expression for the oscillation frequency valid under isothermal conditions and carried out an experimental study of the oscillation frequency as a function of temperature. Since that early work by Atkins, a number of investigators²⁻¹² have studied these oscillations under a variety of experimental conditions. The damping observed during these oscillations was a puzzle to the early workers and the true mechanism is a matter of current discussion.^{8,9,11,13,14} To date at least four possible damping mechanisms have emerged.

One motivation for the work we report here was a desire to understand which of the various damping mechanisms is appropriate. A second motivation was the work of Hammel, Keller, and Sherman,⁵ in which it was reported that during the course of these oscillations a dramatic shift in the frequency of (30-40)% took place in a time of roughly one period of oscillation. The frequency shift they reported was accompanied by a large rise in the decay constant. These results suggested that an unexpected and abrupt change in

ρ_s/ρ or in the film thickness was taking place during the oscillations. In Sec. II we shall describe the damping mechanisms which have been proposed. In Sec. III we describe the apparatus and the techniques used during our measurements. Section IV contains a discussion of our results and a comparison with the various theories of damping. Our conclusions are presented in Sec. V.

II. ISOTHERMAL FREQUENCY AND DAMPING MECHANISMS

In Fig. 1 we display a schematic representation of an apparatus which will support superfluid-film oscillations. We will use its essential features for the present discussion. We assume for the moment that we have isothermal conditions and no dissipation within the moving film. With these assumptions we can neglect the effects of the helium gas and also the fountain effect. The potential energy can be written as

$$V = \int g\rho A_1(1 + A_1/A_2)x dx \quad (1)$$

and the kinetic energy as

$$T = \int \frac{1}{2}\rho_s 2\pi r v^2 \delta dl, \quad (2)$$

where δ is the film thickness at a position l where the flow tube has a radius r . The superfluid moves at local velocity v and the normal fluid is assumed¹⁵ relatively immobile due to its high viscosity. The use of

$$\rho A_1 \dot{x} = 2\pi r \delta \rho_s v \quad (3)$$

allows us to remove v in favor of the rate \dot{x} at which the level in the left reservoir changes. An immediate consequence of neglecting any dissipation process which may take place within the film itself is the equation of motion:

$$\frac{\rho^2}{\rho_s} \frac{A_1^2}{2\pi} \ddot{x} \int \frac{dl}{r\delta} + \rho g x A_1 \left(1 + \frac{A_1}{A_2}\right) = 0 \quad (4)$$

from which we can read off the isothermal frequency,

$$\omega^2 = 2\pi g \frac{\rho_s}{\rho} \left(\frac{1}{A_1} + \frac{1}{A_2}\right) \left(\int \frac{dl}{r\delta}\right)^{-1}. \quad (5)$$

This result was first derived a number of years ago by Atkins.¹ Here the integral is along the film-flow path of perimeter $2\pi r(l)$, g is the acceleration of gravity, and A_1 and A_2 are the free surface areas shown in Fig. 1. The film thickness depends upon the height Z above the free surface at which it is measured. When necessary we shall assume¹⁶ the form $\delta = \xi Z^{-1/n}$. Various measurements¹⁷⁻²⁰ of ξ and n have been reported. Keller¹⁷ has observed that δ is independent of temperature over the range $1.1 \text{ K} < T < T_\lambda$ and thus ω has a temperature dependence given by $(\rho_s/\rho)^{1/2}$.

Now, as we have already indicated, damping is almost always observed in oscillating-film experiments but no mechanism for the damping has been universally accepted. The mechanisms which have been proposed fall into two classes: those which involve a dissipation process in the mobile film itself and one which involves the removal of energy from the oscillations via the reservoirs. We treat these processes by class.

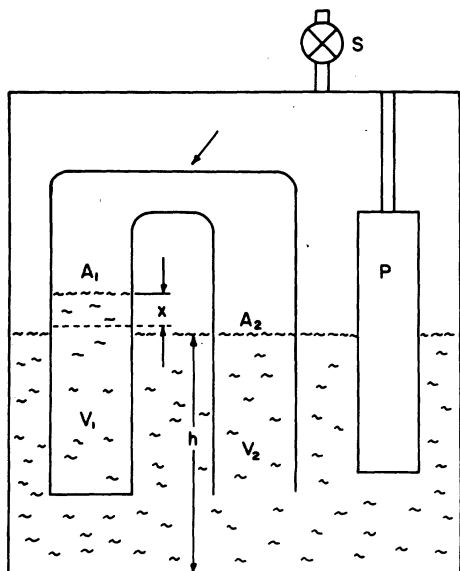


FIG. 1. Schematic representation of an apparatus which will support superfluid-film oscillations. The parameter x represents the displacement from equilibrium of the free surface in the left arm. Level oscillations are induced by the motion of a plunger. The chamber is filled by admitting superfluid helium through a superfluid valve. We refer to this as configuration I.

A. Dissipation in the film

Three mechanisms leading to dissipation in the mobile film have been proposed. The first, due to Allen,¹² assumes that the motion of the film is brought about by an array of vortex lines. Under his hypothesis the scattering of rotons by the vortex array gives rise to a damping force. With the assumption that the strongest temperature dependence in this process is simply the number density of rotons, we are led to the prediction that the superfluid-film oscillations will be damped in a manner such that the damping constant α is related to the number density²¹ of rotons N_R through the expression

$$2\pi\alpha/\Omega \sim N_R \sim T^{1/2} e^{-\Delta/k_B T}, \quad (6)$$

where Ω is the frequency of the oscillation, Δ the roton gap energy,²² and k_B the Boltzmann constant. Several authors^{7,12} have observed that over a limited temperature interval a plot of $\ln\alpha$ vs $1/T$ results in a straight line²³ with slope near Δ/k_B . Since the neglected factor $\Omega T^{1/2}$ does little to change the slope in a $\ln\alpha$ vs $1/T$ plot over the temperature interval $1.2 < T < 2 \text{ K}$, these authors have indicated a more or less favorable comparison with the Allen hypothesis. As we shall describe in detail later, this general agreement is most probably an effect of their experimental geometry and we believe can be understood without recourse to a roton scattering mechanism which operates within the superfluid film.

A second dissipation mechanism which operates within the film was recently proposed by Calvani, Greulich, and Maraviglia.¹³ Their model is based on a suggestion by Feynman²⁴ that the excitations in an accelerated superfluid will tend to orient their momenta antiparallel to the local superfluid velocity. When applied to the case of an accelerated superfluid film, Calvani, Greulich, and Maraviglia (CGM) argue that the alignment process will remove energy from the flow and hence conclude that any accelerated superfluid flow will be dissipative. When applied to the case of film oscillations between two reservoirs, they argue that the energy given up by the film during acceleration is not returned to the film during deceleration. Thus, a damping of the oscillations is to be expected. Under these assumptions they derive an explicit equality for the quantity $2\pi\alpha/\Omega$ which is valid under *isothermal* conditions. They find

$$2\pi\alpha/\Omega = \ln(\rho/\rho_s). \quad (7)$$

Yet another dissipation mechanism which involves the film itself is available. In this mechanism, as developed by Langer and Reppy²⁵ for bulk flow, the flow is limited by the nucleation of

excitations. This dissipation results in a decay of the superfluid velocity v given by

$$dv/dt = -\kappa A f_0 e^{-E/k_B T}, \quad (8)$$

where κ is the quantum of circulation, h/m ; A is the cross-sectional area of the superfluid film, f_0 is an attempt frequency, and E is the energy of the excitation nucleated by the fluctuations. In the consideration of bulk superfluid flows through apertures and channels several authors^{26,27} have chosen the excitation to be a vortex ring in which case $E \sim \rho_s v$. In the case of superfluid films Liebenberg²⁸ and Hoffer *et al.*⁸ have found general agreement with $E \sim \rho_s v$. The work of Hoffer *et al.*⁸ concludes that f_0 is a *dramatic*²⁹ function of temperature. We feel that the quantitative contribution of terms of the form of Eq. (8) awaits precise documentation in the case of the mobile superfluid film. In Sec. IV we will comment further on this point.

B. Dissipation due to the reservoirs

In an attempt to explain dissipation observed in the oscillation of the levels of two reservoirs connected by a superleak (through which bulk superfluid could pass) Robinson³⁰ considered that in any real system which has a finite thermal conductance between the reservoirs one must recognize that temperature oscillations and accompanying fountain pressure oscillations will be a natural consequence of the level oscillations. Under the assumption that superfluid-film oscillations are analogous to bulk oscillations through a superleak, we³¹ have applied the general ideas of Robinson to the specific film-flow configuration given schematically in Fig. 2. When one allows temperature differences to develop between the reservoirs, one must include the effects of both gas-pressure differences and the fountain effect. If we adopt the notation that the two reservoirs can be represented by subscripts as in Fig. 2 we find that the equation of motion for x becomes

$$\frac{A_1}{2\pi} \frac{\rho^2}{\rho_s} \int \frac{dl}{r\delta} \ddot{x} + \rho g \left(1 + \frac{A_1}{A_2}\right) x - (p_2 - p_1) + \rho S'(T_2 - T_1) = 0, \quad (9)$$

where p_1 and p_2 are the gas pressures at the free surface in each reservoir and S' is the entropy deficit $S - S_s$. Here S_s is the entropy of the superfluid component. In the two-fluid model, S_s is strictly zero. Measurements in a number of laboratories indicate that to within experimental error S_s is zero and hence we take $S' = S$. To make further progress we require another equation. A

consideration of the conservation of entropy results in an equation for reservoir 1:

$$\frac{C_P}{T_0} \frac{dT_1}{dt} = -\frac{A_1 S}{V_1} \dot{x} - \frac{K_K(T_1 - T_0) + K_G(T_1 - T_2)}{T_0 \rho V_1}, \quad (10)$$

where we have assumed (i) that the level oscillations are small in amplitude and hence V_1 (the volume of He II in reservoir 1) satisfies $V_1 \gg A_1 x$ and (ii) that heat flow into reservoir 1 takes place by Kapitza-limited conductivity through the detector walls and by the small transfer of mass via gas flow.³² In these equations K_K is the Kapitza-process conductance and K_G is the gas-process conductance. Under the further assumption that the two reservoirs have the same volumes V_0 and conductances K_K , we may introduce the relative temperature ϵ and take $T_1 = T_0 + \epsilon$ and $T_2 = T_0 - \epsilon$. We have then

$$\frac{C_P}{T_0} \dot{\epsilon} + \frac{A_1 S}{V_0} \dot{x} + \frac{K_K + 2K_G}{T_0 \rho V_0} \epsilon = 0. \quad (11)$$

The use of

$$p_1 - p_2 = (T_1 - T_2) dp/dT \quad (12)$$

and our definition of ϵ in Eq. (9) allows a complete

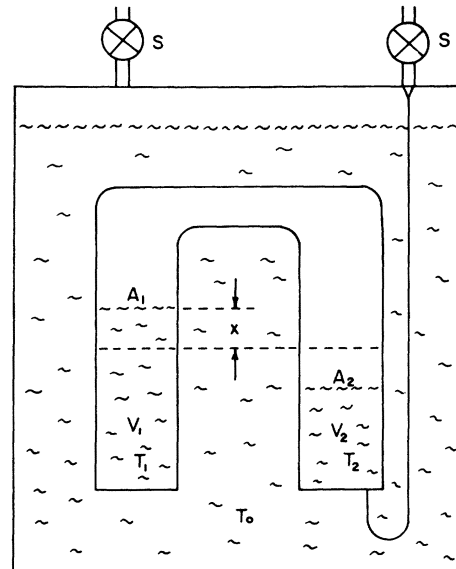


FIG. 2. Schematic representation of an apparatus for which the helium is entirely contained within a sealed environment. Here x again represents the displacement from equilibrium of the free surface in the left reservoir. The chamber and reservoirs are filled through separate superfluid valves. In this configuration (II) all of the flow surfaces are immersed in superfluid. Level oscillations are induced in this case by the application of dc voltages to the coaxial capacitor (not shown) in the right arm as described in the text.

solution for x as a function of time. To facilitate this we adopt the definitions

$$\tau = (C_P/T_0 S)(V_0/A_1)\epsilon, \quad (13)$$

$$\psi = \frac{T_0 S^2 A_1}{g C_P V_0} \left(1 + \frac{A_1}{A_2}\right)^{-1} \left(1 - \frac{1}{\rho S} \frac{dp}{dT}\right), \quad (14)$$

and

$$L = (K_K + 2K_G)/\rho V_0 C_P = K/\rho V_0 C_P, \quad (15)$$

where K is the net conductance. Thus, we have

$$\ddot{x} + \omega^2 x - 2\psi \omega^2 \tau = 0 \quad (16)$$

and

$$\dot{x} + \dot{\tau} + L\tau = 0. \quad (17)$$

These equations are formally identical to those derived by Robinson³⁰ for bulk flow through a superleak. Now τ can be removed in favor of x to reveal

$$\ddot{x} + L\ddot{x} + \omega^2(1 + 2\psi)\dot{x} + L\omega^2 x = 0. \quad (18)$$

This equation has general solutions of the form

$$x(t) = C_1 e^{-\xi_1 t} + C_2 e^{-\xi_2 t} \sin(2\pi\nu t + \phi). \quad (19)$$

Our experimental conditions are such that over our entire temperature range for the parameters of this work we have $\xi_1/\xi_2 > 100$ from Eq. (18). Hence to excellent approximation we have

$$x(t) = C_2 e^{-\xi_2 t} \sin(2\pi\nu t + \phi). \quad (20)$$

Over most of the temperature range of our experiments it is possible to reduce the third-order equation to one of second order¹¹ of the form

$$\ddot{x} + (\omega^2/L)(1 + 2\psi)\dot{x} + \omega^2 x = 0. \quad (21)$$

For our apparatus this predicts decay constants and observed frequencies only a few-percent different from those predicted by Eq. (18) over the temperature range we have studied. Other approximations are also possible.^{8,9} We wish to emphasize that in this work *all* comparisons between our observations and the Robinson theory have been made using solutions [Eq. (19)] to the complete third-order equation [Eq. (18)].

The presence of a finite thermal conductance K between the two reservoirs thus leads to a damping of the superfluid-film oscillations. We will show later that for temperatures below 2 K both the magnitude and temperature dependence of the decay constant as determined in our measurements are well represented by Eq. (18). We will also discuss the crucial importance of the thermal conductance K and suggest that a number of published measurements made over the past decade of the temperature dependence of the decay constant appear consistent with the Robinson theory

once an appropriate apparatus-dependent K is taken into account. Thus, our conclusion will be that the dominant factor in the damping observed in superfluid-film oscillation experiments performed under quasi-isothermal conditions is the small departure from isothermal conditions brought about by the level oscillations themselves.

III. EXPERIMENTAL APPARATUS

It is best to divide a discussion of the apparatus into (i) general features and (ii) the details of the detectors used to study the level oscillations. We begin with the general features. The Dewar was a standard Pyrex model with an inside diameter of 4 in. A Pyrex T was placed at the top so as to allow ready pumping of the helium bath without causing the top plate of the Dewar insert to cool below room temperature. The insert was of standard design with radiation shields placed at suitable intervals along its length. Shielded electrical leads were made using microcoaxial cable^{33,34} and nonshielded leads were made of manganin.

The basic idea of the measurements to be carried out required two reservoirs of helium which were connected by only the mobile superfluid film. An accurate measure of the helium levels in the reservoirs as a function of time is essential for any quantitative comparison with theory. A simple procedure which can be followed to accomplish this measurement which has been followed by a number of investigators recently is to make each reservoir the annular region of a coaxial capacitor. Changes in capacitance then serve to indicate changes in level within a given reservoir. Figure 3 illustrates the basic design we have used for most of the work we report here. We note that this design as shown is equivalent to the configuration (II) shown schematically in Fig. 2. Replacement of the electrical feedthrough on the right with one which is perforated allows operation in the configuration (I) sketched in Fig. 1. The outer shell serves as a grounded shield. Construction (Appendix A) is from oxygen-free high-conductivity (OFHC) copper with the inner and outer electrodes separated by 0.004 in. through the use of Mylar³⁵ tabs. Superfluid integrity is maintained by the use of indium seals. Feedthroughs incorporate the design first described by Anderson.³⁶ The outer electrodes are isolated from the upper arm by means of Mylar³⁵ gaskets with double indium seals. The total capacitance for detectors of this type is 47 pF and a level change of 1 mm results in a capacitance change of 0.092 pF. Building vibrations and acoustical noise limit our resolution of level changes to about $\pm 150 \text{ \AA}$. For our experiments both a ther-

momenter and a heater were located in each level detector. The heaters were 800- Ω coils of No. 45 manganin wire. The detector thermometers were $\frac{1}{10}$ -W nominal 39- Ω Allen-Bradley³⁷ carbon composition resistors and were matched so as to have nearly identical resistance characteristics from 1 K to T_λ . The heaters and thermometers were used primarily in conjunction with direct measurements of the thermal conductance between the two reservoirs.

A stable thermal environment was maintained during the course of these measurements by the combined use of a carefully insulated (from room-temperature variations) regulator of the Walker type and electronic temperature stabilization of the main Dewar. Over the life of an oscillation temperatures were typically controlled to about 1 μ K although on several occasions a stability of 0.3 μ K/h was possible. It was under these conditions of the highest-temperature stability that we were able to observe¹¹ the tiny temperature oscillations associated with the oscillations in fluid levels. The main thermometer (Allen-Bradley, $\frac{1}{2}$ W, nominal 33 Ω) was immersed in the superfluid which partially filled the chamber located at the end of the Dewar insert. This chamber also contained the level-measuring apparatus and a vapor-pressure cell (Fig. 4). The feedback control heater was located *outside* the chamber since this location gave about three times better stability.

Primary temperature calibration was accom-

plished by calibrating the Allen-Bradley resistors by comparison to the vapor pressure of ^4He . For the pressure measurements we used McLeod (10^{-5} –10 Torr) and Wallace and Tiernan (0–120-in. H_2O) gauges. A slight zero correction (0.5 Torr) was applied to the Wallace and Tiernan measurements as determined by a comparison to the McLeod gauge. All of our resistors were cycled to 4.2 K at least three times prior to their first use and calibrations from run to run agree to within a few mK. Calibrations taken during the course of a given run indicated that the shifts over the course of any run were $\ll 1$ mK. The resistance measurements of the main thermometer were made using ac techniques and a Wheatstone bridge. Differential measurements between the reservoirs were made using the symmetric resistors located in the two detectors by employing a carefully shielded bridge. Power dissipation during our resistance measurements was below 10^{-8} W. No effects due to heating could be observed by varying the power.

All superfluid level measurements are three-terminal ac capacitance measurements which employ a General Radio 1615A capacitance bridge (982 Hz, 15 V rms) and a Princeton Applied Research HR-8 as a null detector. Local heating due to this measuring technique does not represent a problem. Signals from the off-null of the PAR HR-8 were recorded in both analog and digital forms. The analog output was obtained through use of an HP 7004A x - y recorder used in the time- y mode.

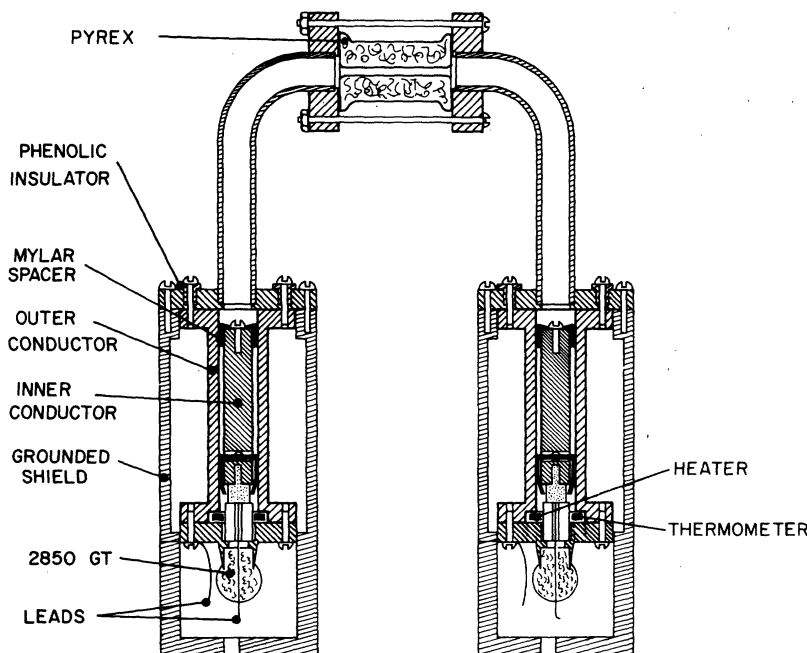


FIG. 3. Actual oscillation apparatus. The Pyrex channel is one of the several constrictions which have been used to limit the oscillation amplitude (see Table I). Operation in configuration I is accomplished by placing holes in the electrical feedthrough structure on the right side. In configuration II a fine capillary is introduced through the feedthrough in the absence of the perforations. The inner conductors are centered through the use of Mylar spacers.

The same signal used to obtain the analog recordings was digitized using a Teledyne-Philbrick 4703A voltage-to-frequency converter and a Monsanto 1500A frequency counter backed through an interface unit by a Tally 420 paper-tape punch. The oscillations we shall present shortly have characteristic periods of 40–60 sec and hence 300 msec was used as a lock-in time constant. No visible changes (aside from slightly more noise) were observed using a 100-msec time constant. Analysis of the recorded data provided by the Tally 420 was carried out directly by computer. Analysis of the chart recordings required an additional step: the traces were first digitized using measuring machines customarily used to analyze bubble-chamber photographs.³⁸

The actual procedures followed during the cool down on our various investigations are described in Appendix B. This description is relevant since the change in configuration from I to II resulted in a necessary change in procedure which may have had a bearing on the quality of our flow surface. We will discuss this point further in Sec. IV and also in Appendix B.

Since our general interest in this work was to study the oscillations of the superfluid film between two reservoirs, some means to initiate the oscillations must be available. We have used two basic techniques: the motion of a plunger in the larger reservoir (configuration I) and the applica-

tion of a dc voltage to one of the capacitors (configuration II). By adjusting the cross section of the plunger nearly any desired level change can be accomplished. Alternatively, if we denote the voltage applied as V a level change³⁹

$$x \approx \frac{\pi \epsilon_0 V^2 (K-1)(K+2)}{3\rho g A \ln(b/a)} \quad (22)$$

is produced as a result of the application of V . Here K is the dielectric constant of helium, and b and a are the outer and inner radii, respectively, of the annulus of cross-sectional area A . We assume here configuration II with equal reservoirs. Voltages of a few hundred volts result in x values of several hundred micrometers. We should point out here that we have also initiated level oscillations by the application of a few microwatts of power to one of the heaters. Since we were interested in a stable thermal environment however, the stimulation of oscillations by the heater was not used during any serious data acquisition. Amplitude calibrations were obtained by measuring the response to a known plunger displacement in configuration I. In configuration II known indentations on the inner conductors were used. Our measurements showed a linear level vs capacitance relationship over the capacitance range used for the oscillations. (See Appendix A.)

A few comments concerning errors are in order. Our ability to determine the decay constant and frequency of these oscillations was limited by building vibrations and acoustical noise. At low temperatures where peak oscillation amplitudes were typically $300 \mu\text{m}$ we could determine α and Ω to better than 1%. At temperatures above 2 K, however, the peak amplitude of the oscillations is severely diminished ($<5 \mu\text{m}$) and in addition the decay constant is at a maximum. These two facts limit our ability to determine α and Ω to within a few percent at these temperatures.

IV. RESULTS AND INTERPRETATIONS OF THE DATA

An example of a level change and subsequent oscillation of the sort typical of our work is shown in Fig. 5. Two general characteristics are evident: a high-velocity segment we shall refer to as the *run-in* during which the helium level moves towards its new equilibrium position after the motion of the plunger or a change in the dc voltage and a segment of lower velocities which we shall refer to as the *oscillation* during which the helium level oscillates about the new equilibrium position. During the run-in the flow sustained by the film is of the type traditionally referred to as critical. As we shall describe briefly here, the flow during the run-in appears consistent with

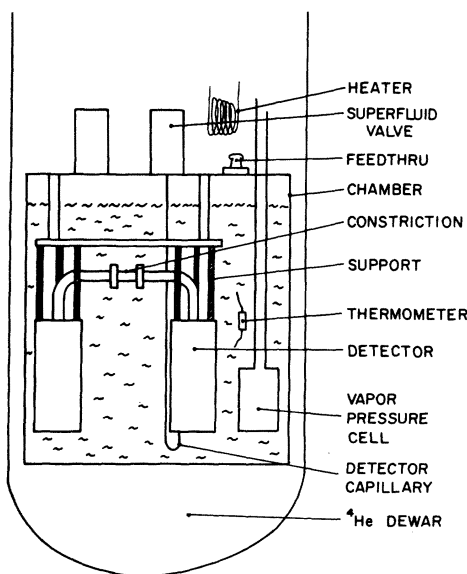


FIG. 4. Basic environment for these experiments. Shown here is the experimental chamber, the detector assembly outline, and the vapor-pressure thermometer. The main resistance thermometer is located inside the chamber, the feedback heater outside.

fluctuation-nucleation²⁵ effects.

That we may separate a discussion of the oscillations from the run-in may not be entirely obvious. To show the motivation for this we refer to Fig. 6 and note that deviations from dissipation-free flow can be examined by studying the dependence of the undamped equation on a parameter such as \dot{x} . Thus, if $\ddot{x} + \omega^2 x = 0$ were the complete equation of motion satisfied by the oscillation and run-in used to produce Fig. 6, then Fig. 6 would be a straight line along the x axis. What we observe instead is a set of points which suggest that in fact terms of the form $A\dot{x} + B \exp(-C/|\dot{x}|)$ are appropriate to the superfluid flow. Hence, the equation of motion may be written

$$\ddot{x} + 2\alpha^* \dot{x} + \epsilon^* (\dot{x}/|\dot{x}|) e^{-B/|\dot{x}|} + \omega^2 x = 0. \quad (23)$$

Hoffer *et al.*⁸ were the first to suggest that an equation of this form is appropriate. Clearly one may evaluate the decay constant α for any trace by fitting to a plot such as Fig. 6. This, in our case is no more accurate than the procedure we have adopted because it requires a second differentiation of the original data. Our procedure has been to confine our attention to the oscillation region and fit our data for x to a function of the form

$$x(t) = A e^{-\alpha t} \sin \Omega t. \quad (24)$$

To guarantee that this procedure be successful we must begin our fits far enough down the decay of

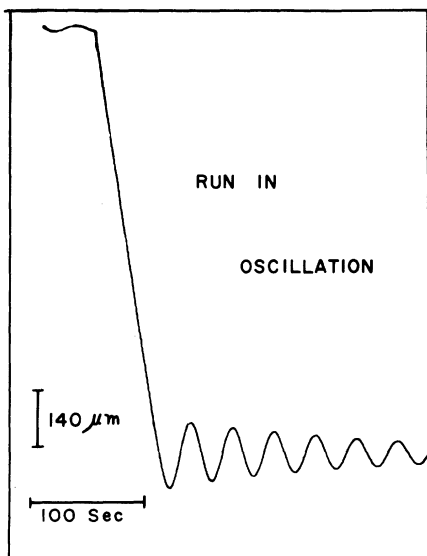


FIG. 5. Typical film-flow trace. The approach to equilibrium (run-in) takes place at a finite velocity apparently governed by processes within the film. Oscillations about equilibrium follow the run-in and are damped. The character of the run-in depends on the constriction in use.

the oscillation so that we are guaranteed $|\dot{x}|_{\max}$ is small enough to make the term linear in \dot{x} the major factor in the observed dissipation. Within our ability [by direct computer fits of the data to Eq. (23)] to determine the effect of the exponential term, we find that its⁴⁰ effect is always negligible for our apparatus after about one cycle of the oscillation. This then is the technique we have used to determine α and Ω and hence the undamped frequency $\omega = (\Omega^2 + \alpha^2)^{1/2}$.

Now the processes which give rise to the fluctuation damping are expected to take place predominantly in those regions of the apparatus where the superfluid velocity is the largest. Our experiments have been conducted using geometries for which the high film velocity region is well localized. Various constrictions have been placed in the flow path as detailed in Table I. In particular, we have examined differences in the high-velocity run-in between long channel constrictions and aperture constrictions. This study has not been completely analyzed and we reserve the details for a future publication.

Since the Robinson theory as applied to film oscillations contains the thermal conductance, quantitative comparison to the theory requires that K be determined for each experimental configuration. The thermal conductance can be measured for various equilibrium levels of He II by using (e.g., the left side) a heater to establish a temperature difference. Thus, given a known heat input per second, \dot{Q} , we measure the resulting temperature difference ΔT and hence $K = \dot{Q}/\Delta T$. Extensive measurements of K have been carried out at various

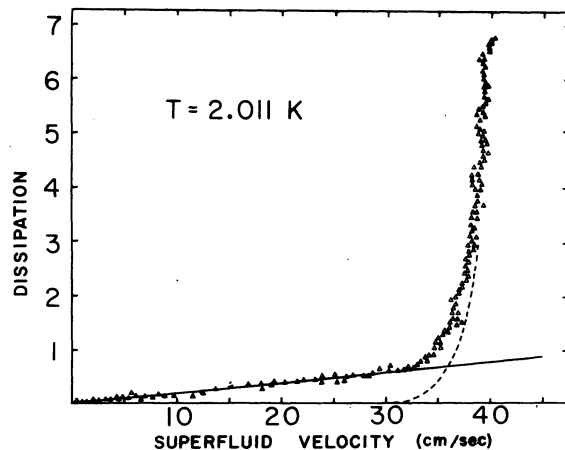


FIG. 6. Dissipation vs velocity of the superfluid film. We have plotted here $|\ddot{x} + \omega^2 x|$ vs $|\dot{x}|$. Finite values indicate that the two terms $\ddot{x} + \omega^2 x$ are not adequate to describe the motion. In particular we see the need for a term linear in \dot{x} and another which rises steeply at large values of \dot{x} .

TABLE I. Various constriction types we have studied. The dimensions are given in inches. In this work we report in detail the results of oscillation studies using the last two constrictions. The letters *A*, *B*, and *C* are explained in the text.

Material	Diameter	Thickness	Text Code
Copper	0.093	0.0015	...
Nickel	0.007	0.001	...
Nickel	0.020	0.001	...
Nickel	0.040	0.001	...
Pyrex	0.040	0.040	...
Pyrex	0.060	0.040	...
Pyrex	0.040	0.450	A,B
Pyrex	0.060	0.450	C

temperatures and various equilibrium helium levels inside our detectors. Figure 7 displays the measured temperature dependence of K for a value of the helium level characteristic of most of the data we present here. K is weakly dependent on the level of the liquid in the detector as might be expected. Changes in K over level changes associated with the oscillations amount to less than 0.1% and have been neglected.

We should point out that we have obtained the ΔT

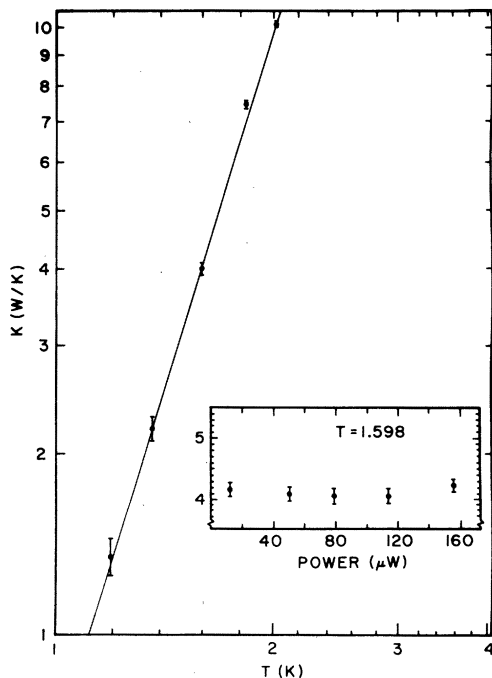


FIG. 7. Thermal conductance K for our apparatus as a function of temperature. The inset shows the conductance at a particular temperature as a function of heater power. Typically, heat was applied to the left arm while the right arm remained at the ambient chamber temperature.

values used in our determination of K from the fountain effect rather than from our direct observations of the applied differential temperature. This is simply due to the fact that our ability to measure level differences exceeds our ability to directly measure equivalent temperature differences. As indicated in Table II, our directly measured temperature differences were consistent with the temperature differences deduced from the fountain effect. Table II is characteristic of all of our measurements. The values of K presented in Fig. 7 are insensitive to different values of \dot{Q} at each temperature studied (over the \dot{Q} range studied, $3 \times 10^{-6} - 2 \times 10^{-4}$ W). An example of this lack of sensitivity to \dot{Q} is shown in the inset on Fig. 7. Thus, we have confidence that our values for $K(T)$ are reliable.

An additional measure of the thermal properties of our apparatus has been obtained by causing the temperature inside (e.g., the left) detector to differ from that outside by the application of a steady constant amount of heat. Removal of this heat source causes the temperature of the helium inside the detector to drop to the bath value in some time τ_0 ($1/e$ value). Measurements of τ_0 show that $\tau_0 \approx 20$ msec. This is consistent with calculations of τ_0 which take into account the Kapitza resistance between the helium and the copper wall of our detector. Since the period of the oscillations we have observed are all in excess of 38 sec, the rate of superfluid transport is small enough to allow us to estimate that the maximum temperature excursions which take place in a given detector as a result of the level oscillations are $(\Delta T)_{\max} \approx 0.5 \mu\text{K}$. The thermometers present allow a measurement of the differential temperature during the level oscillations to an accuracy of about $\pm 0.3 \mu\text{K}$ under the best circumstances. Under these conditions we have seen¹¹ very small temperature oscillations which accompany the level oscillations. In no case have we ever observed a differential temperature oscillation between the two reservoirs to be greater

TABLE II. Conductance values as a function of heater power at a particular temperature. Here we compare the directly measured temperature difference with that deduced from the fountain effect. As discussed in the text, the fountain ΔT values are more accurate.

Power (μW)	Level (μm)	Fountain ΔT (μK)	Measured ΔT (μK)	K (W/K)
3.2	28.	0.43	0.35	7.43
12.7	110.	1.66	1.06	7.65
28.6	244.	3.69	4.59	7.75
50.6	445.	6.71	6.71	7.54
79.4	695.	10.48	10.95	7.58

than 1.2 μK peak to peak under normal operating conditions. These differential temperature amplitudes are seen only in conjunction with differential level amplitudes with peak-to-peak values of $\approx 400 \mu\text{m}$. These temperature oscillations are of an amplitude consistent with predictions based on the Robinson theory and their detection supports our evidence that the Robinson theory applied to film flow in the presence of finite conductance correctly describes the oscillation damping.

With these comments in mind, we proceed to a discussion of the oscillations. To begin we note that in none of these studies^{10,11} have we seen strong frequency shifts or decay-constant peaking of the sort reported in Ref. 5. Changes in temperature, constriction size, and material and detector assembly were carried out and none of these produced pronounced frequency shifts and large decay-constant changes. While strong-frequency shifts (over a time scale of the order of one cycle of oscillation) have *never* been observed in our measurements, gradual shifts which amount to a percent or so over the lifetime of a complete oscillation are often visible. It is interesting to speculate as to the source of these drifts and we do so in Appendix C. Part way through the course of this work it was suggested⁴¹ that a leak may have been responsible for the shifts reported in Ref. 5. During one run we accidentally made a faulty indium seal in configuration I at the place indicated by the arrow in Fig. 1. This resulted in a competing parallel path for the superfluid flow into and out of our detector. The presence of this leak (which represented an extra perimeter of roughly the same dimensions as the Pyrex aperture in use at the time) did not result in a strong-frequency shift from one stable value to another. It did, however, result in a frequency instability in the oscillations. The conclusion is that multiple superfluid-film paths can affect the oscillation frequency in a way which is not completely understood at present.

We now present data from three specific experimental investigations. The first, *A*, utilized configuration I and the relevant parameters are given in Table I. In the second, *B*, the *only* change was to go to configuration II. No changes in the geometry were made. In the third, *C*, again configuration II was used but in this case a different constriction was employed and also the "dead" volume of liquid in the detectors was reduced by 50% by the addition of nylon chips. These changes all result in changes in the frequency of the superfluid-film oscillations. In particular, they allow us to test the functional dependence of the decay constant on frequency. Both the Allen¹² hypothesis and that due to Calvani, Greulich, and Maraviglia¹³ suggest a linear dependence whereas the Robinson

theory predicts $\alpha \sim \omega^2$. Our experimental results for α and $\omega = (\alpha^2 + \Omega^2)^{1/2}$ are shown in Figs. 8 and 9. Again, α and Ω are obtained from fits of the data by Eq. (24). All of the points shown in our figures represent average values of the quantity displayed. These averages were typically obtained from six to ten events at each temperature.

The smooth curves drawn through the data in the frequency plots have been drawn with the temperature dependence of $(\rho_s/\rho)^{1/2}$ and normalized at one point. This has been done since we do not know precisely (i) the film profile $\delta = \xi/Z^{1/n}$ and (ii) the exact nature of the flow surface. These missing pieces of information make a quantitative comparison between Eq. (1) as applied to our geometries and the data of Fig. 9 somewhat uncertain. In spite of this, if we *assume* that $n=3$ in the expression for the film profile and we *assume* the flow surfaces are well represented by the macroscopic geometry, we extract from the frequency data an effective value of ξ for the three measurements as $4.1 \times 10^{-6} \text{ cm}^{4/3}$ (*A*), $5.1 \times 10^{-6} \text{ cm}^{4/3}$ (*B*), and $4.6 \times 10^{-6} \text{ cm}^{4/3}$ (*C*). We associate about a $\pm 40\text{-}\text{\AA}$ uncertainty with each value. According to Eq. (1) we should expect the frequency ω to increase by approximately $\sqrt{2}$ when we go from configuration I to II. We observe instead a shift of a factor of about 1.5. We attribute this increase to the small apparent thickening of the film caused by slight

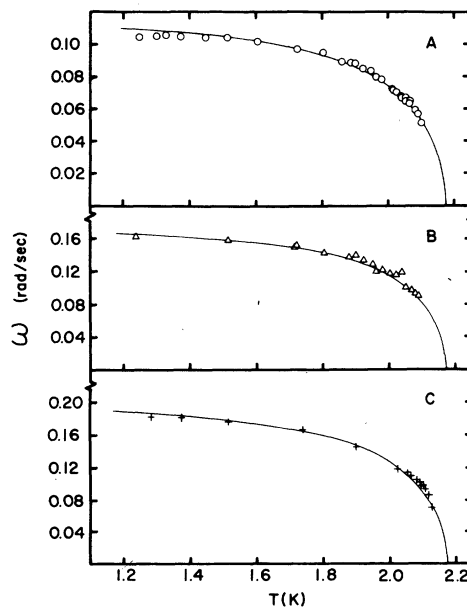


FIG. 8. Derived frequency $\omega = (\alpha^2 + \Omega^2)^{1/2}$ vs temperature. The smooth curves have the temperature dependence of $(\rho_s/\rho)^{1/2}$. *A*, *B*, and *C* refer to the three experiments described in the text. Here α and Ω are experimental values from fits by Eq. (24).

flow surface contamination. This was a result of the requirement of evacuating the reservoirs through a small capillary as discussed in Appendix B. Subject to cautions previously mentioned, we accept $\xi = 4.1 \times 10^{-6} \text{ cm}^{4/3}$ as the clean surface value for our apparatus. It is interesting to note that this value lies between the values for our constriction materials $\xi = 4.0 \times 10^{-6}$ (glass) and 4.3×10^{-6} (copper) as calculated by Schiff.⁴² Measured values of ξ as reported¹⁷⁻²⁰ in the literature vary rather widely. Subject to the uncertainties we have discussed, our value for ξ seems about 25% larger than measurements by a number of workers. This value is, however, in substantial agreement with that obtained by Keller¹⁷ for a stainless-steel surface. Figure 10 is a plot of ω^2 vs ρ_s/ρ for these experiments which, according to Eq. (1), should be a straight line in each case.

The smoothed curves drawn through the decay-constant figures, Fig. 9, are a result of using Eq. (18) and the *experimental* undamped frequency values $\omega = (\alpha^2 + \Omega^2)^{1/2}$. Except for the region near T_λ we observe that the agreement between theory and experiment is quite good. It should be noted

again here that for temperatures above 2.0 K the oscillation amplitude is very small and vibrational noise limits the accuracy with which we can make determinations of α and Ω . For example, the oscillations had a peak-to-peak amplitude of 300 μm in the vicinity of 1.3 K and only 1 μm at 2.13 K. We note that the difference between the measurements of α (A and B) at a given temperature scale roughly⁴³ as ω^2 . This fact can be seen more clearly by reference to Fig. 11 where we plot α vs $1/T$. This plot is in striking resemblance to similar plots^{7,12} which have been presented in the literature. The straight-line character over most of the temperature interval has, in our opinion nothing to do with a behavior governed by $\exp(-\Delta/k_B T)$, but rather is a simple consequence of the fact that any strong dependence *looks* exponential over a severely limited range of the parameter of interest. Specifically, the smooth curves are again a result of the Robinson theory. If one demands a behavior like $\exp(-\Delta/k_B T)$, one finds $\Delta/k_B = 10.9 \pm 0.2 \text{ K}$ as compared to the roton gap of $\Delta/k_B \sim 8.6$. A plot of $2\pi\alpha/\Omega$ (Fig. 12) further displays this disagreement with the Allen hypothesis. Since our results were

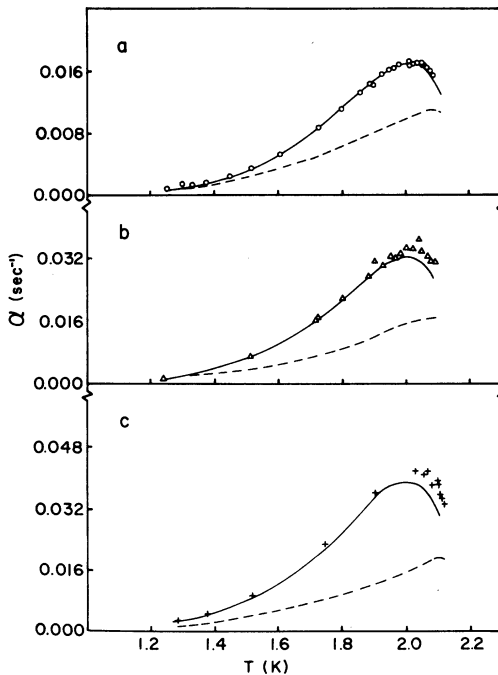


FIG. 9. Experimental damping vs temperature. The derived $\omega = (\alpha^2 + \Omega^2)^{1/2}$ values have been used in Eqs. (16) and (17) to produce the solid curves. The Robinson theory describes the damping very well for temperatures below 2 K. The dashed curves represent the contribution to the damping which would be present if the polarization process (see text) suggested by Calvani, Greulich, and Maraviglia were in operation.

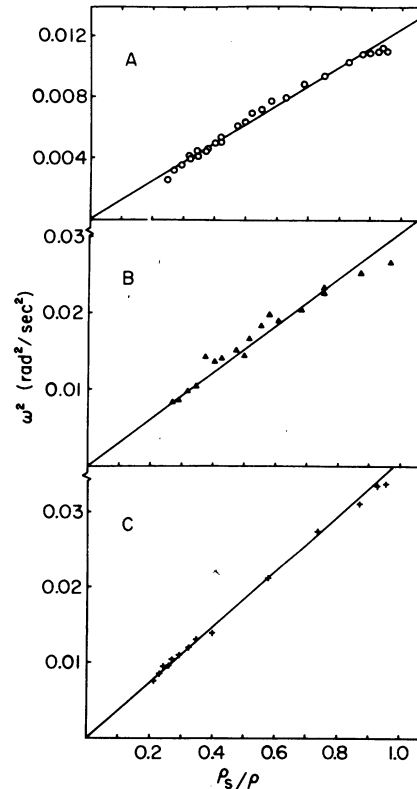


FIG. 10. Derived frequency $\omega^2 = \alpha^2 + \Omega^2$ vs ρ_s/ρ . According to the Robinson theory as applied to our experimental apparatus, this should be a straight line. Slight systematic deviations are seen.

not carried out under perfectly isothermal conditions we cannot explicitly test the apparatus independence of Eq. (3). However, since the mechanism proposed by Calvani, Greulich, and Maraviglia¹³ involves the film itself, it should operate *in addition* to the Robinson mechanism. Given our observed frequency Ω a contribution to α given by $\alpha_{\text{CGM}} = (\Omega/2\pi) \ln(\rho/\rho_s)$ should be present in the observed damping if the CGM process is at work. The expected CGM contribution is shown as a dashed line in Fig. 9 along with our data and the Robinson prediction. Since the Robinson theory is in *quantitative* agreement with experiment for $T < 2$ K, we conclude that the mechanisms proposed by both Allen¹² and by Calvani, Greulich, and Maraviglia¹³ either do not contribute to the damping at all in this temperature range or else provide a very small contribution compared with the mechanism originally proposed by Robinson. Above 2 K we observe a damping of the oscillations which is somewhat in excess of that given by the Robinson theory. Although as we have indicated, accurate measurements are difficult in this temperature

region, we believe the departures may be real. We have not yet established a complete quantitative confirmation of the mechanism involved.

We now turn to a closer look at the Robinson theory and predictions which can be based on it. In particular we focus attention on the thermal conductance K . For the experiments we have reported here, this quantity is adequately described by a power law which is consistent with Kapitza-limited heat flow through the copper walls of our reservoirs. A small contribution to the conductance, however, is due to viscous limited flow to helium gas which is distilled and condensed as a result of the small but finite-temperature fluctuations which accompany the level oscillations. Allen, Armitage, and Saunders⁹ have observed film oscillations which they describe in terms of the Robinson theory for which the gas conductance mechanism was a *dominant* contribution. They also pointed out that their results were not in conflict with the Allen hypothesis since they could obtain $\Delta/k_B \approx 9$ K from their measurements. Our own results *are* in conflict with the Allen hypothesis and quantitative agreement with our measurements is only available from the Robinson theory. In our view the previous consistency with the roton-scattering mechanism was simply the result of the particular experimental conditions (geometry, K , etc.) and the fact that these experiments are conducted over a very narrow range of $1/T$. As we detail in Appendix D, when the gas conductance

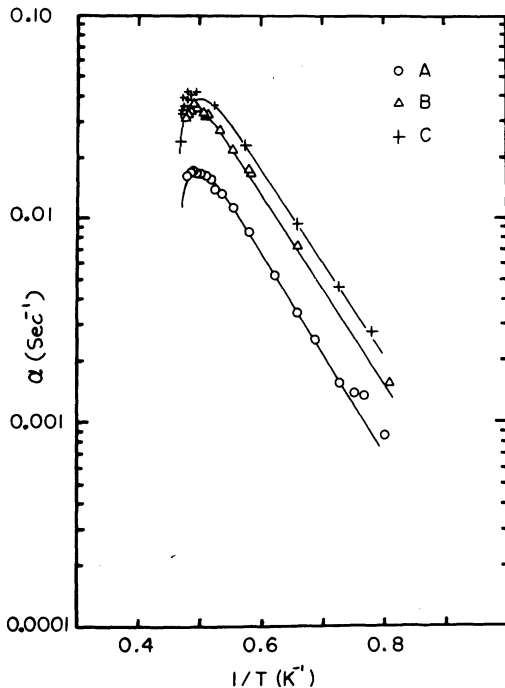


FIG. 11. A traditional plot of the decay constant vs inverse temperature. As detailed in the text, we believe that the linearity evidenced here is *not* associated with roton scattering. The letters refer to the experiments we have described. Note that the change from configuration I (data A) to configuration II (data B) resulted in very nearly a factor-of-2 shift in α at each temperature as expected on the basis of the Robinson theory.

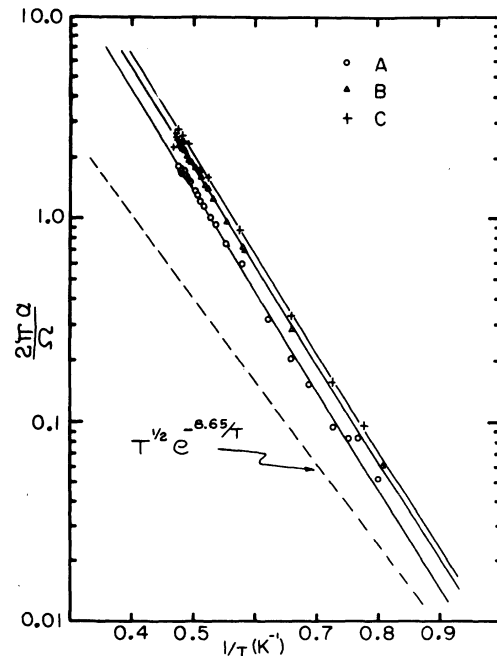


FIG. 12. $2\pi\alpha/\Omega$ vs inverse temperature.

mechanism is dominant and limited by gas viscosity its effect may produce a qualitative difference in the temperature dependence of the decay constant over that observed when the distillation process governs the conductance. Further measurements of the temperature dependence of α over a wider range of temperatures and conductance conditions would be very useful.

V. CONCLUSION

We have demonstrated that the Robinson theory as applied to superfluid-film flow between two reservoirs is capable of describing our experimental observations of the damping of the oscillations both with regard to the dependence of α on frequency as well as on temperature. These results are consistent with earlier considerations of the Robinson theory given by Hoffer *et al.*,⁸ and Allen, Armitage, and Saunders.⁹ We are convinced that the mechanism due to Calvani, Greulich, and Maraviglia is of *minor* importance in our observations. We expect that their claim that the excitation polarization mechanism is capable of explaining previous experimental results is *invalid*. Similarly we are convinced that the roton-scattering process first described by Allen is of minor importance for the conditions of our observations. In particular, we believe that previous general agreement with predictions based on the Allen hypothesis has simply been the result of the experimental geometries employed and the limited temperature range of the studies. This view is supported by proper Robinson predictions for the slope of $\ln(2\pi\alpha/\Omega)$ vs $1/T$ for our measurements and similar predictions of a different slope when the theory is applied to the different experimental conditions reported by others. (See Appendix D.)

ACKNOWLEDGMENTS

We are indebted to W. E. Keller and M. E. Banton for several stimulating discussions and an enthusiastic interest in our work. J. K. Hoffer pointed out the utility of plots such as Fig. 6 to us. We are indebted to R. R. Kofler for his suggestions in reducing the data using the measuring machines. G. Good of the University Glass Shop deserves thanks for his efforts in fabricating the Pyrex constrictions. Special thanks are due R. Galkiewicz for his enthusiastic assistance with some of the computer analysis and H. Robkoff for his construction of the interface to the paper tape punch. We are also indebted to F. Hmura and W. Piela for their skillful machining of the capacitors.

APPENDIX A: DETECTOR CONSTRUCTION

Here we describe the basic procedures we have used to produce the inner and outer conductors of our capacitive level detectors. Both conductors were machined from oxygen-free high-conductivity (OFHC) copper rods. The inner conductors were carefully lathe turned and subsequently polished. The outer conductors received more special treatment. They were drilled out and reamed on a lathe. The inside surface was then polished by forcing a precision steel ball down its axis using a lubricant.⁴⁴ By starting with a ball of the size of the reamed hole and increasing the size (by a few 0.0001 in.) on subsequent forcings a high quality surface can be obtained. Over the 3-mm length which we used to conduct these measurements the inner conductors were measured⁴⁵ to be uniform in diameter to 2500 Å (the accuracy of the air gauge used to perform the measurement). Over the same length the outer conductors had a measured inside diameter uniform to 5000 Å.

APPENDIX B: COOLDOWN PROCEDURES

We outline here the basic procedures used during a cooldown in configuration I and then describe the differences required for configuration II. The apparatus in configuration I was inserted in the room-temperature Dewar and the chamber was pumped by a nitrogen-trapped diffusion pump for 48 h, sufficient time to cause an ionization gauge between the chamber and the nitrogen trap to plateau (few $\times 10^{-6}$ Torr). The chamber was then flushed several times with helium gas purified by a Linde⁴⁶ 13X molecular sieve at 77 K by raising the chamber pressure to 1 Torr. This was followed by an additional 24 h of pumping during which the ionization gauge again reached a plateau. Cooldown to 77 K was then accomplished with 1 atm of ⁴He gas in the glass Dewar helium space. After ⁴He-liquid transfer was initiated the superfluid valve leading to the chamber was opened briefly to admit gas to the level-measuring apparatus. Later the chamber was filled to the operating level. These precautions seemed adequate to prevent contamination of the flow surfaces by air.

The fill capillary employed in configuration II required differences from the just described procedure. Prior to the 48-h pumping period the detector assembly was flushed the order of 10 times with helium gas purified by 13X at 77 K. At the 48-h point several flushes to 1 Torr were accomplished followed by a 24-h pumping. The plateaus reached in this case were somewhat more gradual as might be expected. Also, since the detector assembly was to be filled via its own valve, helium

gas was allowed in the large chamber at all stages. After ${}^4\text{He}$ -liquid transfer and $T < T_\lambda$ helium was admitted to the detector assembly by condensation of 13X purified ${}^4\text{He}$ gas in a coil in the main Dewar bath. As we indicate in the main text, this evacuation procedure may have been responsible for some contamination of the flow surfaces.

APPENDIX C: FREQUENCY STABILITY

As we have discussed, on no occasion did we ever observe strong frequency shifts of the sort seen by Hammel *et al.*⁵ An accidental leak in one experiment allowed us to study the effect of a multiply connected flow path on the frequency. The frequency measured under these conditions was sometimes noisy with apparently random fluctuations occurring a number of times during the decay of an oscillation. Multiply connected flow paths appear to affect the oscillations in a complicated way which we do not completely understand at present.

One specific example deserves mention. On several instances we observed what appeared to be a reasonably normal run-in and oscillation upon raising the plunger. Upon lowering the plunger several minutes later we initiated a run-in in the opposite direction but almost no oscillation was visible. This strong asymmetry was quite reproducible at the helium level and temperatures at which it was observed. We have never observed such a dramatic asymmetry in our usual, simply connected geometries.⁴⁰ Further experiments along these lines may be interesting.

We do generally see gradual frequency shifts of a percent or so over the life of an oscillation. These shifts are not always precisely reproducible but their regular presence leads us to believe that they may have a physical basis and we shall now explore that point in some detail. The expression we have written for the oscillation frequency under undamped conditions, Eq. (5), will be very nearly the actual frequency of oscillation, Ω , at low temperatures (since $\alpha \ll \Omega$). In particular, we should notice the presence of the position-dependent film thickness in this expression. Keller¹⁷ has directly observed that this thickness does not depend on velocity. If that is in fact true, the frequency should remain constant over the lifetime of a complete oscillation to equilibrium (assuming ρ_s/ρ remains constant). If, however, Kontorovich⁴⁷ is correct, the thickness of the film at any given height z above the superfluid bath will be given by

$$\delta(v, z) \approx \delta_0(1 + \rho_s v^2 / 2\rho g z)^{-1/3}, \quad (25)$$

where δ_0 is the film thickness at a height z under $v=0$ conditions. Now, v can be simply related to

\dot{x} and observed by our techniques by geometrical considerations and the conservation of mass [see Eq. (3)].

The simple observation that $\langle \dot{x}^2 \rangle$ is a monotonically decreasing function of time when averaged over successive periods of oscillation for damped harmonic motion leads us to the conclusion that if the film thickness is in fact governed by Eq. (25) then a measurement of the frequency on subsequent periods of oscillation for the damped oscillations will result in a nonconstant frequency due to the *average* thickening of the film as the oscillation diminishes. Thus, on subsequent periods the frequency will rise.

We have measured the frequency stability for a large number of oscillations and find results reasonably consistent with expectations obtained by inserting Eq. (25) into (5) as a function of v . The absence of complete reproducibility in observing these ($\approx 1\%$) frequency shifts over the life of the oscillations cautions us against premature conclusions. A separate apparatus designed to maximize the effect of Eq. (25) is in operation in an attempt to settle the question. *Preliminary* results from this new apparatus at 1.2 K are consistent with the predictions of Kontorovich. As yet we have neither established the possible temperature dependence⁴⁸ of our observations nor have we carefully examined the role of the quality⁴⁹ of the flow surface.

APPENDIX D: THERMAL CONDUCTANCE VIA THE GAS

Thermal contact between two reservoirs of He II via mass transport can be understood by a consideration of two important effects (i) evaporation of atoms from the fluid surface in the warmer reservoir and (ii) viscous flow of the helium gas in the tubes which lead to the colder reservoir. For the moment we shall ignore the possibility that for isothermal flow tubes the atoms in the warmer gas may be deposited on the mobile film. Evaporation effects in He II have been studied in some detail by Atkins, Rosenbaum, and Seki.³² A detailed consideration of the effects of evaporation and viscosity-limited flow leads to the following expression for the thermal conductance

$$K_c = L \frac{Q^* dp/dT}{1 + (2Q^*/A_0)(2RT/M)^{1/2}}. \quad (26)$$

Here L is the latent heat per gram for the evaporation process, R the gas constant, M the molecular weight, dp/dT the temperature derivative of the vapor-pressure curve, and A_0 the effective area of the fluid surface in our (here assumed equal) detectors. It is important to note that A_0 is generally not the same as the geometric cross-section

tional surface area. Q^* is the effective viscous conductance of the tubes which support the gas flow. In general for conductances in series

$$1/Q^* = \sum_i 1/Q_i, \quad (27)$$

where Q_i is the conductance for a given segment of the flow path. For example, for a straight tube we have⁵⁰

$$Q_i = (\pi/8) \rho r^4 / \eta l, \quad (28)$$

where r is the radius and l the length of the channel. Here η is the viscosity⁵¹ and ρ the density of the helium gas.⁵²

The conductance due to this mechanism is thus an interplay between the number of atoms made available by the evaporation process and the ability of the flow tubes to transport these atoms. An example of this interplay for a specific experimental configuration is shown in Fig. 13. The specific conductivity in a given experiment will have a strong effect on the decay constant pre-

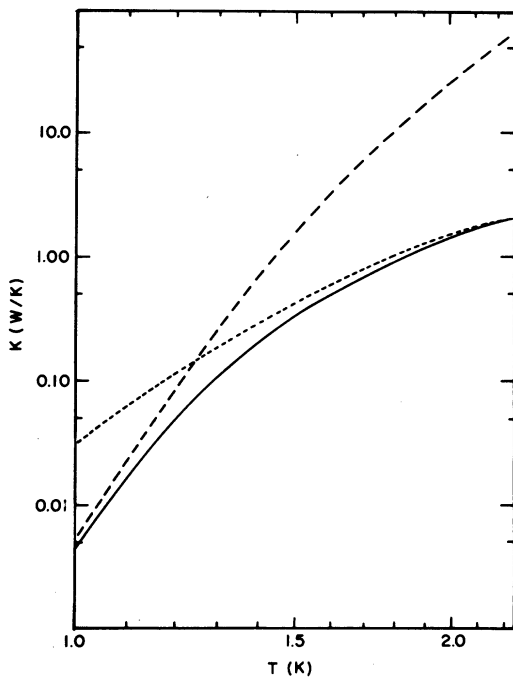


FIG. 13. Conductance vs temperature as calculated using the gas-conductance mechanism for a geometry similar to configuration II. In this example viscosity effects limit the conductance (— — —) at low temperatures and the distillation process limits the conductance (—) at high temperatures. In the absence of a Kapitza-limited conductance process, the total conductance from this mechanism can lead to a leveling off of the Robinson damping at low temperatures if the conditions are right.

dicted by the Robinson theory. Specifically, we have shown the predictions of the Robinson theory as applied to our geometry and measured conductance values in Figs. 9 and 11. If we calculate the decay constant expected on the basis of the Robinson theory as applied to the Pyrex geometry used by Allen under the assumption that the gas conductance dominates, we obtain the result shown in Fig. 14. For temperatures above 1.2 K this has a "slope" $\Delta k_B \approx 8.6$ in reasonable agreement with the measurements of Allen, given our uncertainties concerning the geometry of Allen's⁵³ apparatus. Of particular interest is the predicted leveling of the decay constant at lower temperatures when viscosity effects limit the conductivity. That this is a possibility appears to have been first suggested by Martin.⁵⁴ It should be noted here that Martin's measurements indicate a slope of about 4.5 on a plot of $\ln \alpha$ vs $1/T$. This result differs from any others reported and appears *outside* the scope of the Robinson theory. At present no explanation for Martin's observation is available. This leveling may be an explanation for the saturation observed by Bianconi and Maraviglia⁷ in the vicinity of 1 K although their *apparent* geometry was not really consistent with viscous limited flow as a dominant process.

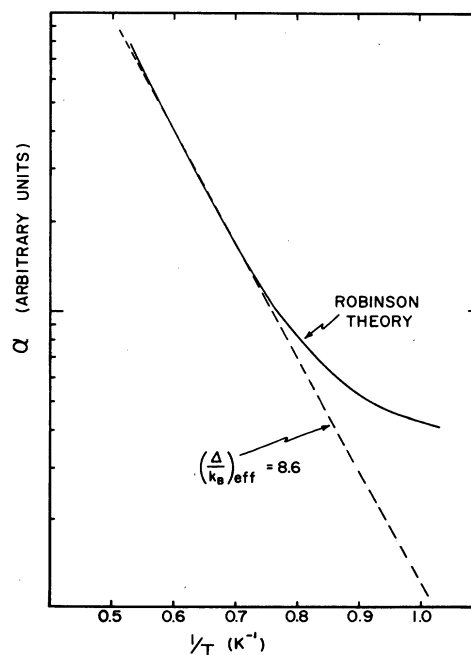


FIG. 14. Decay constant as calculated from the Robinson theory using the geometry of Allen. For this calculation the gas-conductance mechanism is assumed dominant. Note that for temperatures from about 1.2 to 2 K the Robinson theory gives an *apparent* slope Δ/k_B very much in agreement with Allen's hypotheses.

- *Supported by the National Science Foundation (GH-34534) and during the initial phases also by the Research Corporation (Cottrell Grant). Computation facilities were provided by the University Computation Center.
- †Alfred P. Sloan Fellow.
- ¹K. R. Atkins, Proc. R. Soc. A203, 119 (1950).
 - ²G. S. Picus, Phys. Rev. 94, 1459 (1954).
 - ³H. Seki, Phys. Rev. 128, 502 (1962).
 - ⁴F. I. Glick and J. H. Werntz, Jr., Phys. Rev. 178, 314 (1969).
 - ⁵E. F. Hammel, W. E. Keller, and R. H. Sherman, Phys. Rev. Lett. 24, 712 (1970).
 - ⁶D. J. Martin and K. Mendelssohn, J. Low Temp. Phys. 5, 211 (1971).
 - ⁷A. Bianconi and B. Maraviglia, J. Low Temp. Phys. 1, 201 (1969).
 - ⁸J. K. Hoffer, J. C. Fraser, E. F. Hammel, L. J. Campbell, W. E. Keller, and R. H. Sherman, in *Proceedings of the Thirteenth International Conference on Low-Temperature Physics, Boulder, Colo., 1972*, edited by R. H. Kroppschot and K. D. Timmerhaus Plenum Press, New York.
 - ⁹J. F. Allen, J. G. M. Armitage and B. L. Saunders, *ibid.*, Ref. 8.
 - ¹⁰R. B. Hallock and E. B. Flint, Phys. Lett. A 45, 245 (1973).
 - ¹¹R. B. Hallock and E. B. Flint, Phys. Rev. Lett. 31, 1383 (1973).
 - ¹²J. F. Allen, *Proceedings International School of Physics, Course No. XXI—Liquid Helium*, edited by G. Careri (Academic, New York, 1963), p. 305.
 - ¹³P. Calvani, R. Greulich, and B. Maraviglia, Nuovo Cimento Lett. 6, 536 (1973).
 - ¹⁴R. B. Hallock and E. B. Flint, Phys. Lett. A 47, 417 (1974).
 - ¹⁵This assumption is valid here since the saturated film thickness is much smaller than the viscous penetration depth which is about 10 000 Å.
 - ¹⁶The precise form of the helium-film profile depends on the substrate which supports it and apparently also on the surface preparation of that substrate.
 - ¹⁷W. E. Keller, Phys. Rev. Lett. 24, 569 (1970).
 - ¹⁸A. C. Ham and L. C. Jackson, Proc. R. Soc. A240, 243 (1957).
 - ¹⁹L. G. Grimes and L. C. Jackson, Philos. Mag. 48, 1346 (1959).
 - ²⁰E. S. Sabisky and C. H. Anderson, Phys. Rev. A 7, 790 (1973).
 - ²¹See, for example, *Experimental Superfluidity*, R. J. Donnelly (University of Chicago Press, Chicago, 1967), p. 78.
 - ²²D. G. Henshaw and A. D. B. Woods, Phys. Rev. 121, 1266 (1961); R. A. Cowley and A. D. B. Woods, Can. J. Phys. 49, 177 (1971).
 - ²³Deviations from this straight-line relationship have also been noted. In particular see Ref. 7 and also D. J. Martin, Ref. 54.
 - ²⁴R. P. Feynman, Phys. Rev. 94, 262 (1954).
 - ²⁵J. S. Langer and J. D. Reppy, *Progress in Low Temperature Physics* (edited by C. J. Gorter, North-Holland, Amsterdam, 1970), Vol. 6, p. 1-35. The original concepts were developed by S. V. Iordanskii, Zh. Eksp. Theor. Fiz. 48, 708 (1965) [Sov. Phys.—JETP 21, 467 (1965)] and J. S. Langer and M. E. Fisher, Phys. Rev. Lett. 19, 560 (1967).
 - ²⁶H. A. Notarys, Phys. Rev. Lett. 22, 1240 (1969).
 - ²⁷S. J. Harrison and K. Mendelssohn, *ibid.*, Ref. 8.
 - ²⁸D. H. Liebenberg, Phys. Rev. Lett. 26, 744 (1971).
 - ²⁹In particular, in Ref. 8, it was reported that f_0 changed by 10^{23} as the temperature changed from roughly 1 K to roughly T_λ . This dramatic change is not observed in a preliminary analysis of our own high-velocity data.
 - ³⁰J. F. Robinson, Phys. Rev. 82, 440 (1951).
 - ³¹The Robinson theory has previously been applied to film flow by others in a more approximate way. See Refs. 8 and 9.
 - ³²K. R. Atkins, B. Rosenbaum, and H. Seki, Phys. Rev. 113, 751 (1959).
 - ³³Available from Uniform Tubes, Incorporated, Collegeville, Pa.
 - ³⁴E. B. Flint and R. B. Hallock, Rev. Sci. Instrum. 44, 1133 (1973).
 - ³⁵E. I. du Pont de Nemours Company, Wilmington, Dela.
 - ³⁶A. C. Anderson, Rev. Sci. Instrum. 39, 605 (1968).
 - ³⁷Available from Reliance Merchandising Company, Philadelphia, Pennsylvania.
 - ³⁸These machines have a stated accuracy of 0.001 in. over 4 ft. and were much more accurate than our ability to follow the chart recording trace.
 - ³⁹See, for example, W. K. H. Panofsky and M. Phillips, *Classical Electricity and Magnetism* (Addison Wesley, Reading, Mass.), p. 112.
 - ⁴⁰We should note here that we sometimes observe an anomalously large *first* peak in the oscillation which does not appear to be consistent with the fluctuation effects as described in Eq. (23). This presence (Ref. 5) of "enhanced damping" depends on the previous history of the film and when present is usually asymmetric between the two possible run-in directions. (See also Appendix C).
 - ⁴¹W. E. Keller (private communication).
 - ⁴²L. I. Schiff, Phys. Rev. 59, 839 (1941).
 - ⁴³Evidence for a scaling as ω^2 in a single experiment for different path lengths has been presented in Ref. 9.
 - ⁴⁴Do All No. 150 light oil (nonsulfur), Do All Corporation, Hartford, Conn.
 - ⁴⁵These measurements were carried out by Westfield Gauge Company, Westfield, Mass.
 - ⁴⁶Linde is a division of the Union Carbide Corporation.
 - ⁴⁷V. M. Kontorovich, Zh. Eksp. Theor. Fiz. 30, 805 (1956) [Sov. Phys.—JETP 3, 770 (1956).]
 - ⁴⁸E. van Spronsen, H. J. Verbeek, R. de Bruyn Ouboter, K. W. Taconis, and H. van Beelan, Phys. Lett. A 45, 49 (1973). [See also, R. de Bruyn Ouboter, J. Low Temp. Phys. 12, 3 (1973).]
 - ⁴⁹M. E. Banton and W. E. Keller have observed that the magnitude of the apparent film thinning seen in experiments of the sort reported by G. A. Williams and R. E. Packard [Phys. Rev. Lett. 32, 587 (1974)] may depend on the surface quality of the flow surface over which the helium moves; private communication.
 - ⁵⁰See, for example, R. D. Present, *The Kinetic Theory of Gases* (McGraw-Hill, New York, 1958).
 - ⁵¹R. A. Buckingham and R. A. Scriven, Proc. Phys. Soc. Lond. A65, 376 (1952).
 - ⁵²W. E. Keller, *Helium 3 and Helium 4* (Plenum, New York, 1969).
 - ⁵³J. Allen (private communication).
 - ⁵⁴D. J. Martin, Ph.D. dissertation (Oxford University, 1969) (unpublished).